IEEE Access
Multidisciplinary ⋮ Rapid Review ⋮ Open Access Journal

Received 15 March 2023, accepted 24 March 2023, date of publication 29 March 2023, date of current version 14 April 2023.

Digital Object Identifier 10.1109/ACCESS.2023.3262985

RESEARCH ARTICLE

Multiple Autonomous Surface Vehicles for Autonomous Cooperative Navigation Tasks in a Marine Environment: Development and Preliminary Field Tests

JEONGHONG PARK[1], (Member, IEEE), MINJU KANG[1], (Member, IEEE), YEONGJUN LEE[2], (Member, IEEE), JONGDAE JUNG[3], (Member, IEEE), HYUN-TAEK CHOI[1], (Member, IEEE), AND JINWOO CHOI[1], (Member, IEEE)

[1]Advanced-Intelligent Ship Research Division, Korea Research Institute of Ships and Ocean Engineering (KRISO), Daejeon 34103, Republic of Korea
[2]Ocean and Maritime Digital Technology Research Division, Korea Research Institute of Ships and Ocean Engineering (KRISO), Daejeon 34103, Republic of Korea
[3]Department of Naval Architecture and Ocean Engineering, Chungnam National University (CNU), Daejeon 34134, Republic of Korea

Corresponding author: Jinwoo Choi (jwchoi@kriso.re.kr)

This work was supported by the Endowment Project (Development of modeling/simulation and estimation/inference technology for digital twin ship) through the Korea Research Institute of Ships and Ocean Engineering under Grant PES4860.

ABSTRACT This paper presents the development and field testing of multiple autonomous surface vehicles (ASVs) for autonomous cooperative navigation tasks in marine environments. The developed ASVs were designed in a catamaran hull form, and various systems related to autonomous functionalities, including the electrical propulsion, wireless communication, and guidance, navigation, and control (GNC) systems, were integrated with the situational awareness sensor system. Because not all of the navigation and situational awareness sensor data can be shared owing to the large network load, the network communication and data protocol structure was designed to enhance the data management efficiency. Furthermore, for cooperative navigation between multiple ASVs, the network communication system was synchronously shared with motion information through a robot operating system (ROS) multi-master system. In particular, an autonomy framework with cooperative navigation and control was designed to enable autonomous cooperative maneuvering with multiple ASVs in a global navigation satellite system (GNSS)-denied environment. Furthermore, a cooperative navigation and control approach based on relative geometric information between vehicles was implemented in the framework, which incorporated the capabilities of following a predefined path and maintaining a specific formation based on the relative distance between ASVs. Moreover, to demonstrate the essential maneuvering and functional capabilities of the cooperative navigation and control approach of the developed ASVs, preliminary field tests were conducted in an inland water environment, and the test results are discussed in this paper.

INDEX TERMS Autonomous surface vehicle (ASV), cooperative localization, cooperative navigation and control, formation control, multiple ASVs.

I. INTRODUCTION

In recent years, industrial demand for autonomous and unmanned systems has increased significantly due to advancements in sensing, embedded systems, and autonomy capabilities. In the maritime sector, many missions are still carried out by humans, resulting in a high risk of casualties. To replace these tasks with marine unmanned systems such as autonomous underwater vehicles (AUVs) and autonomous surface vehicles (ASVs), active research is

The associate editor coordinating the review of this manuscript and approving it for publication was Tao Wang.

underway to develop intelligent and autonomous unmanned systems. Although the capabilities of unmanned systems in performing marine missions are currently limited, the industrial demand for them may increase owing to decreasing employment opportunities [1], [2], [3]. In particular, ASVs have been widely used in various marine missions, including, shallow water surveying, ocean environmental monitoring, oceanography, structural inspection, maritime surveillance, and reconnaissance [4]. Most of these missions have been performed using a single system; however, studies using multiple ASVs have been actively conducted to perform missions more efficiently and expand marine applications with advanced technologies and autonomy capabilities [5]. Cooperative operation using multiple ASVs offers certain advantages for performing multi-objective missions in terms of time efficiency, complementary detection ability, and fault detection and tolerance in comparison with using a single ASV [6]. In addition, new marine missions can be performed by fusing information obtained from individual vehicles and sharing spatial and situational awareness information over a wide area.

To maximize the merits of operating multiple ASVs, certain factors must be considered more technically than when operating a single ASV. In terms of system and device components, each ASV is typically designed to be equipped with interchangeable all-ASV compatible sensors and devices mounted on it. Further, low-cost sensors mounted on each vehicle to implement technologies that can increase efficiency in terms of performance and specifications compared with advanced sensors mounted on a single vehicle must be used. Furthermore, the information obtained and fused in each vehicle must be synchronously exchanged in real time through a configured wireless network system. Hence, a network communication structure and exchanging data protocol must be well organized according to the network system specifications and configuration.

To meet these requirements, multiple systems have been integrated and implemented using a robot operating system (ROS). The topic publishing and subscribing structure provided by a ROS facilitates systematic management and sharing of vital statuses and information messages of multiple systems. However, only one ROS master can exist in a network when applying ROS to multiple robot systems. However, an extension that enables the deployment of multiple ROS masters exists, which is referred to as ROS multi-master [7]. The ROS multi-master extension supports various ROS networks communicating with each other such that it can support multiple robotic systems [8]. Several studies on multi-agent and multi-robot applications using a ROS multi-master have been conducted [9], [10].

To ensure autonomy while achieving the goals of various missions and tasks using multiple ASVs, a cooperative navigation and control framework that enables sharing of mutual information between vehicles must be systematically constructed. The basic framework can be similar to the guidance, navigation, and control (GNC) system of a single ASV. However, cooperative navigation, localization, and formation control technologies must be included in the framework to enable the safe simultaneous operation of multiple ASVs in a harsh environment. When operating multiple ASVs, cooperative navigation technologies must be implemented to address navigation problems caused by global navigation satellite system (GNSS) failures, whether temporary or permanent [11], [12]. GNSS-related navigation problems can occur in real systems owing to several accidental and deliberate reasons, such as hardware and software failures and network system errors [13], [14]. To address these problems, cooperative navigation and localization techniques through information exchange between vehicles have been actively studied [15]. Cooperative localization has been developed for various types of autonomous systems, such as ground mobile robots, aerial vehicles, and marine vehicles. A cooperative positioning system has been proposed for ground mobile robotic systems using three-dimensional (3D) laser scanning to minimize position error accumulation [16]. Further, cooperative localization using heterogeneous robotic systems has also been studied to ensure the cooperation between different types of robots, such as unmanned ground vehicles (UGVs) and unmanned aerial vehicles (UAVs) [17], [18], [19]. In the case of marine applications, cooperative navigation has been extensively studied for various types of multiple autonomous systems. Multiple AUVs have been the subject of several studies on cooperative navigation [20], [21], [22]. Both heterogeneous and homogeneous structures have been investigated for the cooperative navigation of multiple AUVs [23]. Furthermore, research has been conducted on the cooperation between ASVs and AUVs [24], [25], [26], [27]. Cooperative navigation and localization approaches are implemented by sharing data between vehicles, allowing low-accuracy vehicles to be localized using high-accuracy vehicle information.

Furthermore, the cooperative navigation and control framework must comprise key technologies, including formation control to build or transform various specific geometric shapes and collision avoidance between ASVs [28], [29]. To achieve formation maintenance and transformation, various approaches have been proposed, including leader–follower [30], [31], [32], virtual structure (or virtual leader) [33], [34], [35], and behavior-based [36], [37] approaches. Oh et al. [38] proposed the categorization of formation control schemes into position-, displacement-, and distance-based controls according to the types of sensing capabilities and interaction topology. During the maintenance and transformation of specific geometric shapes, the framework design must consider a formation path planning approach, including a collision avoidance strategy between vehicles as well as static or dynamic objects or both [39], [40], [41].

In this study, three ASVs with a cooperative navigation and control framework were developed to implement the fundamental autonomous navigation functionalities required

for advanced marine missions. An autonomy framework with cooperative navigation and control is proposed to estimate the motion information of a vehicle based on an extended Kalman filter (EKF). Relative geometric information between vehicles was used to manage GNSS failures or operate in a GNSS-denied environment. In addition, the autonomy framework was designed to build or transform specific geometric shapes between vehicles based on the hybrid formation control approach, which was fused based on the virtual leader and leader–follower concepts. The three ASVs were divided into one leader and two follower vehicles, and the leader vehicle provided virtual goal waypoints that were followed by each vehicle with formation maintenance by exchanging motion information between vehicles. Further, to implement these autonomous functionalities, each vehicle was built using various hardware modules and software algorithms. Moreover, their feasibility was demonstrated through field tests in an inland water environment.

The remainder of this paper is organized as follows: Section II presents an overall description of the hardware and software architectures of the developed system. Section III presents the autonomy algorithms designed for autonomous cooperative navigation and control. Field experimental results with multiple ASVs in an inland water environment are presented and discussed in Section IV. Finally, Section V summarizes the findings of this study and provides a brief discussion on future research prospects and key aspects to be considered when implementing multiple ASVs in real time and for maritime missions.

II. SYSTEM DEVELOPMENT

A. DESIGN REQUIREMENTS

The reliability and robustness of the developed system should be a fundamental capability for performing allocated mission tasks using multiple ASVs. Each ASV was designed as a catamaran-type hull platform to ensure maneuvering stability and ease of installation. Furthermore, each ASV was equipped with validated commercial-off-the-shelf (COTS) sensors and devices to secure reliability and durability and reduce maintenance costs. To achieve autonomous capabilities, a GNSS-based navigation system and an inertial measurement unit (IMU), as well as a sensor system for situational awareness using a radar, stereo camera, and LiDAR, were installed on each vehicle. In addition, wireless network systems and communication data structures were designed to facilitate simultaneous operation and data transmission between vehicles without network latency in real time. A ROS-based middleware framework enables high compatibility and scalability with systems and autonomy algorithms; this was adopted to implement vehicle autonomy functionalities, including an autonomous cooperative navigation and control framework. Furthermore, it was integrated into each ASV system. Moreover, each ASV was designed to maneuver as an independent vehicle, implying that each vehicle was equipped with autonomous solutions and could handle undesirable situations such as network or system failures of other vehicles within multiple ASVs.

TABLE 1. Specifications of the developed MAIVs.

Designation [unit]	MAIV-1	MAIV-2 & MAIV-3
Length (L) [m]	4.3	4.1
Breadth (B) [m]	2.5	2.1
Platform weight [kg]	400	300
Payload [kg]	up to 300	up to 150
Speed [knots]	up to 6.25	up to 6.75
Propulsion	Two electric thrusters (5 HP each)	
Power	Lithium battery x 3ea (25.9 Vdc / 104 Ah)	
Endurance	8 h @ 3 knots (per charge)	
Onboard computer	Lenova ThinkStation P340 Tiny x 2ea (CPU (i7-10700T), RAM (16GB DDR4), GPU (NVIDIA Quadro P1000))	
Sensors	Stereo camera (Hanwha) Radar (Simrad, HALO24) LiDAR (Ouster, OS1-64) GNSS (Hemisphere, V133) AHRS (Microstrain, 3DM-GX5-25) FOG (Advanced Navigation, Spatial FOG Dual) (only MAIV-1)	

B. HARDWARE ARCHITECTURE

Fig. 1 shows the developed ASVs and the hardware architecture for each vehicle. The ASVs are referred to as mid-scale autonomous and intelligent vehicles (MAIVs) and consist of two types of vehicles; MAIV-1 (Fig. 1(a)) is designated as the leader vehicle, and it is slightly larger than MAIV-2 and MAIV-3 (Fig. 1(b)), which are designated as follower vehicles. The key specifications of the MAIVs equipped with various integrated sensors and devices are summarized in Table 1. To consider the system maintenance efficiency in terms of hardware and software systems, identical key component sensors and devices were integrated into each vehicle. Each vehicle comprised several component units: a battery management system (BMS) with three batteries and a control unit of twin outboard thrusters, a wireless fidelity (WiFi) and emergency (EMC) communication network unit for reciprocal sharing of information, a navigation and situational awareness sensor device unit, and an autonomous navigation and control unit, as shown in Fig. 2.

The onboard computer was integrated with an Intel CPU running Ubuntu and a ROS as the middleware, which implemented data processing related to navigation sensors and control systems. Another onboard computer was used for processing the situational awareness sensor data (e.g., the stereo camera, radar, and LiDAR). In addition, a microcontroller unit (MCU) with an STM32F7 core was integrated to transmit and receive the control command and status data between the onboard computer and BMS/thruster unit. Data were exchanged based on the UART interface. Furthermore, the motion information estimated from the navigation unit of each vehicle was reciprocally shared using a WiFi communication system.

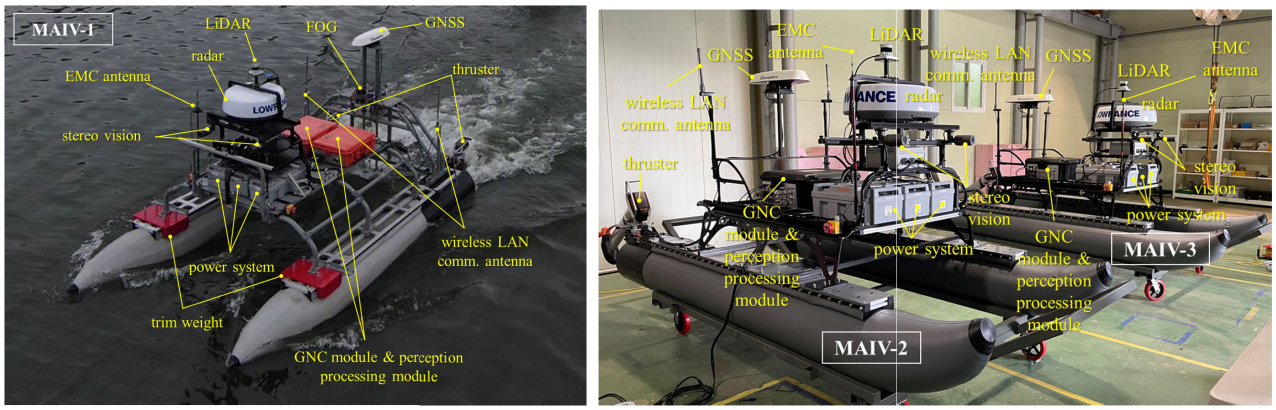

FIGURE 1. Overview of the mid-scaled autonomous and intelligent vehicles (MAIVs) and hardware architecture developed in KRISO: (a) MAIV-1 is used as the leader ASV; (b) MAIV-2 and MAIV-3 are used as the follower ASVs.

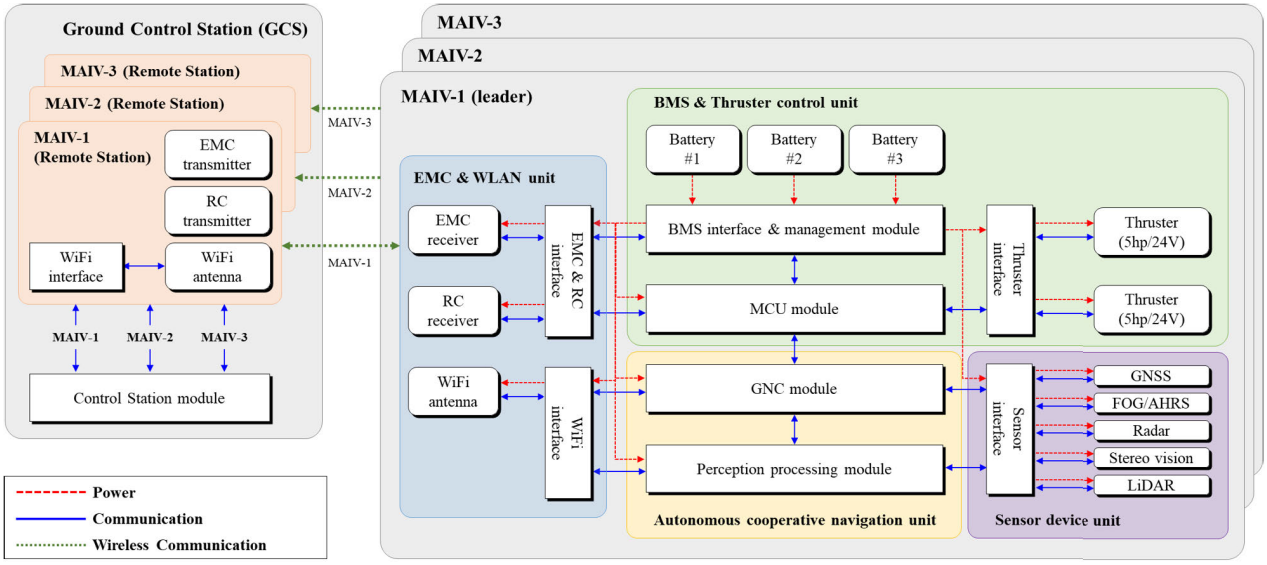

FIGURE 2. Schematic of the hardware architecture of the BMS and propulsion system of the MAIVs, communication system, navigation and situational awareness sensors, and onboard navigation and control system for autonomy. BMS: battery management system; EMC: emergency; GNSS: global navigation satellite system; MCU: micro control unit; RC: remote control; GNC: guidance, navigation, and control; FOG: fiber optic gyroscope; AHRS: attitude and heading reference system.

C. NETWORK ARCHITECTURE

To achieve complementary cooperative capabilities between vehicles, the entire fleet, including the three MAIVs, simultaneously used their mounted situational awareness sensors. In summary, the fleet used three LiDARs, three radars, and three stereo camera systems. Therefore, a large computational and network load was expected on the entire system. Specifically, the network bandwidth required for transmitting point cloud data from a LiDAR as a ROS message is typically 65MB/s, whereas the image data from radar and stereo camera systems may require up to 3.0 MB/s. Given that we have three MAIVs, this amount of bandwidth could potentially cause data loss or significant network delays. To ensure reliable MAIV maneuvers without unstable network latency, the following network design aspects were considered: First, each vehicle must operate independently as a complete system such that it can handle occasional or potential network failures. From a ROS application perspective, this implies that the developed system must operate as its own ROS master environment. Second, each vehicle must have the ability to interact with other vehicles based on a broadcast communication network solution to obtain complementary perception capabilities and perform cooperative missions. Third, a systematic data-sharing structure between vehicles must be established. In particular, because the bandwidth of the wireless network was limited to 1 Gbps, determining the data to share was an important factor in terms of network load.

Hence, to fulfill these design considerations, a data integration structure comprising two sensor fusion stages was applied. The first sensor fusion stage, which merged

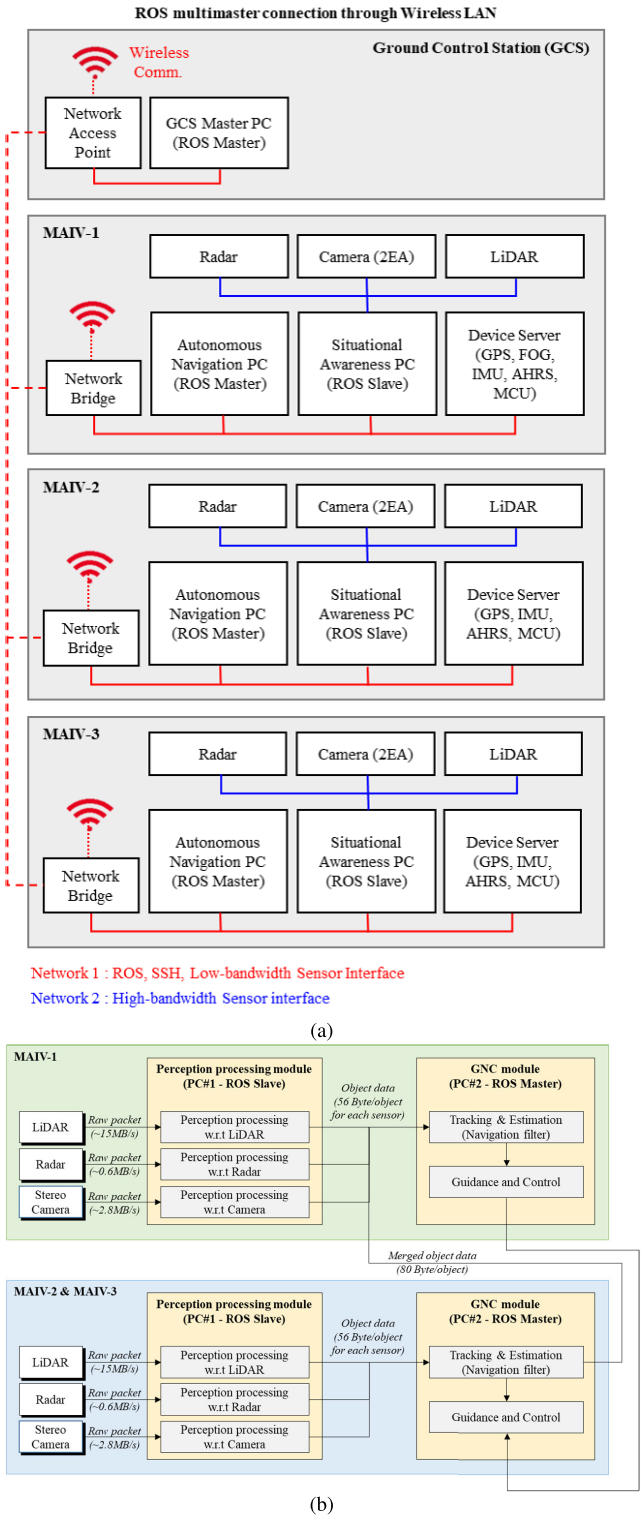

FIGURE 3. Network architecture based on a ROS multi-master configuration with the developed MAIVs: (a) Network structure with respect to low/high-bandwidth sensor interface; (b) Network structure among the processing and GNC modules between the MAIVs.

the perception results of the LiDAR, stereo camera, and radar, was performed in each vehicle system. Subsequently, MAIV-wise sensor fusion was performed based on swarm operation. This structure offered advantages in terms of computational load distribution and network load minimization. Our object detection system for LiDAR, radar, and stereo camera systems was designed to have a capacity of 56 bytes per detected object. During PC-to-PC or MAIV-to-MAIV communication, we did not transfer raw data from detection sensors. Instead, the sensor-wise object detection results were fused with the MAIV-wise object results, which had a capacity of 80 bytes per detected object. The final result of the MAIV-wise object detection was then transmitted to the leader MAIV through wireless communication and fused into the fleet-wise object detection results. Fig. 3 shows the network structure of the MAIVs. A more detailed explanation with the formulation is addressed in Section III.B.

In terms of software implementation, we used ROS as a main development framework. ROS is a powerful middleware platform for improving the development efficiency of various autonomous systems. It is designed to have a graph architecture composed of a set of nodes, and each node refers to a unit process that covers from low-level device control to the implementation of high-level algorithms. In the developed system, those sensor device units, BMS and thruster control unit, the EMC and WLAN unit, and autonomous cooperative navigation unit operated as individual nodes. Software integration was accomplished by publishing and subscribing messages between nodes, and communication between nodes was governed by the ROS master operating on each MAIV. Connection and data transfer between nodes were implemented using the ROS API to ensure user convenience. In the developed system, the ROS multi-master was adopted to address the aforementioned considerations. A multi-master enabled multiple ROS systems to manage and communicate with each other without affecting the ROS network of each system [7]. Consequently, each vehicle remained an independent system while being fully compatible with the other vehicles. In addition, all data, including navigation, control, and perception information, were shared throughout the network system configured for each vehicle.

D. SOFTWARE ARCHITECTURE

The primary design requirement of the software architecture was reliable and robust algorithms in all operating situations. The developed software involved hardware interface modules, and autonomous algorithms were implemented in C/C++ for real-time maneuvering and operation.

The software components comprised two modules: an intelligent situational awareness (iSA) module and a GNC module. The iSA module for intelligent situational awareness was implemented for sensor data processes, including data logging, unit conversion, object detection and tracking, and the delivery of processed information to the GNC module. Because two high-resolution cameras, LiDAR, and radar data processing exert a large computational load on a single computer, data processing latency can occur. Thus, preprocessing techniques that reprocessed the raw data received from each

situational awareness sensor were used to consider an efficient computational processing load.

A GNC module includes the guidance, navigation, and control algorithms for implementing autonomy capabilities associated with cooperative navigation and control tasks. The module carries data through various device interface components to the propulsion and emergency systems as well as control commands received from a ground control station (GCS). Here, in the cooperative navigation and control unit, a localization approach corresponding to GNSS-denied situations was incorporated based on the relative geometric information between vehicles, as described in Section III-B. The cooperative control unit included two maneuvering capabilities: waypoint guidance and tracking and formation control approaches, which are described in detail in Sections III-A and III-C, respectively.

III. AUTONOMOUS COOPERATIVE NAVIGATION AND CONTROL FRAMEWORK

The GNC module framework for cooperating with autonomous navigation and control between MAIVs is shown in Fig. 4. In the navigation unit, a cooperative navigation approach based on relative geometric information was designed to prevent navigation problems derived from GNSS failure and degradation and GNSS-denied situations. Further, a cooperative guidance and control approach in the guidance and control unit facilitated the adoption of a desired geometric pattern between multiple vehicles by sharing estimated information from the navigation unit. The proposed approaches for the designed cooperative framework are described in detail next.

A. WAYPOINT GUIDANCE APPROACH

The autonomous navigation framework for cooperative navigation between MAIVs was designed based on the formation control scheme through the fusion of the virtual leader and leader–follower approaches. The leader MAIV-1 generated and provided virtual waypoints to build the predefined formation of the MAIV fleet using the motion information of the follower MAIVs. Subsequently, the generated waypoints were assigned as the goal waypoint of each MAIV, and a guidance and control approach for rapidly following the goal waypoint and concurrently minimizing the errors corresponding to line-of-sight (LOS) and cross-track (CT) is preferentially required. Thus, a waypoint tracking guidance and control scheme was individually implemented for each vehicle.

Because the platform type of each vehicle was developed as a nonholonomic system, it was assumed that the motion model of each vehicle could be simplified as a three-degree-of-freedom (3-DOF) system, as shown in Fig. 5. Moreover, the proposed LOS guidance approach was modified and applied to minimize the LOS error corresponding to the angle of the direction from which the vehicle was heading toward the goal waypoint. A general LOS guidance approach involves creating a virtual circle around the vehicle to guide its direction. The performance of this approach is highly dependent on the size of the virtual circle chosen. In our implementation, the size of the virtual circle was determined based on the goal waypoint, ensuring that the LOS of the vehicle always pointed toward it. The LOS error between the ith vehicle and its goal waypoint was calculated as $\psi_{i,e} = \psi_i - \psi_{i,los}$, where $\psi_{i,los} = tan^{-1}((y_{i,los} - y_i)/(x_{i,los} - x_i))$. In contrast, the CT guidance approach was employed to minimize the CT error corresponding to the perpendicular distance from the straight line between the previous and current goal waypoints to the current position of the vehicle. The CT error was calculated as $d_{i,cte} = \left(\sqrt{(x_{i,los} - x_i)^2 + (y_{i,los} - y_i)^2}\right) sin\alpha$, where $\alpha = tan^{-1}((y_{i,los} - y^p_{i,wp})/(x_{i,los} - x^p_{i,wp})) - \psi_{i,e}$. The guidance approach was designed such that wherever the position of the vehicle was, $x_{i,los}$ and $y_{i,los}$ were set to $x^c_{i,wp}$ and $y^c_{i,wp}$ as the current goal waypoints.

B. COOPERATIVE LOCALIZATION

1) LOCALIZATION OF A SINGLE VEHICLE UNDER NORMAL CONDITIONS

MAIVs that move on the water surface can utilize GNSS to acquire current positions. The developed vehicle was equipped with an onboard GNSS and IMU to estimate the position and attitude of the vehicle. Further, a localization system for each vehicle performed fusion processing with the GNSS and IMU to estimate its 3D location and attitude under normal conditions. The localization process through GNSS and IMU fusion was designed and implemented using an EKF framework. The state vector of the EKF for pose estimation is defined in (1).

$$\mathbf{x} = \left[\, x, y, z, \phi, \theta, \psi, u, v, w \right]^\top \tag{1}$$

here x, y, and z represent the 3D positions, ϕ, θ, and ψ represent the 3D attitude of the vehicle, and u, v, and w represent the body-fixed frame velocities of the vehicle. Although MAIVs move on the water surface, they can also experience heave, roll, and pitch motions. Hence, the localization process should estimate 3D position and attitude, as defined in (1).

As a traditional EKF-based tracking filter scheme, the proposed localization filter comprised prediction and correction steps. In the prediction step, the IMU was used to predict the motion information, which is defined as a kinematic model of the vehicle (2).

$$\hat{\mathbf{x}}(t) = f(\mathbf{x}(t-1), u_t) \tag{2}$$

here $f(\cdot)$ is the kinematic model of the vehicle and u_t is the control input for time t. In the proposed method, u_t represents the sensor data measured from the IMU, which includes the three accelerations $(a_x,\ a_y,\ a_z)$ along with the three angular velocities $(\omega_x,\ \omega_y,\ \omega_z)$ at time t (3).

$$u_t = \left[\, a_x,\ a_y,\ a_z,\ \omega_x,\ \omega_y,\ \omega_z \right]^\top \tag{3}$$

The uncertainty in the current vehicle state is represented by the covariance matrix in the EKF localization framework. The

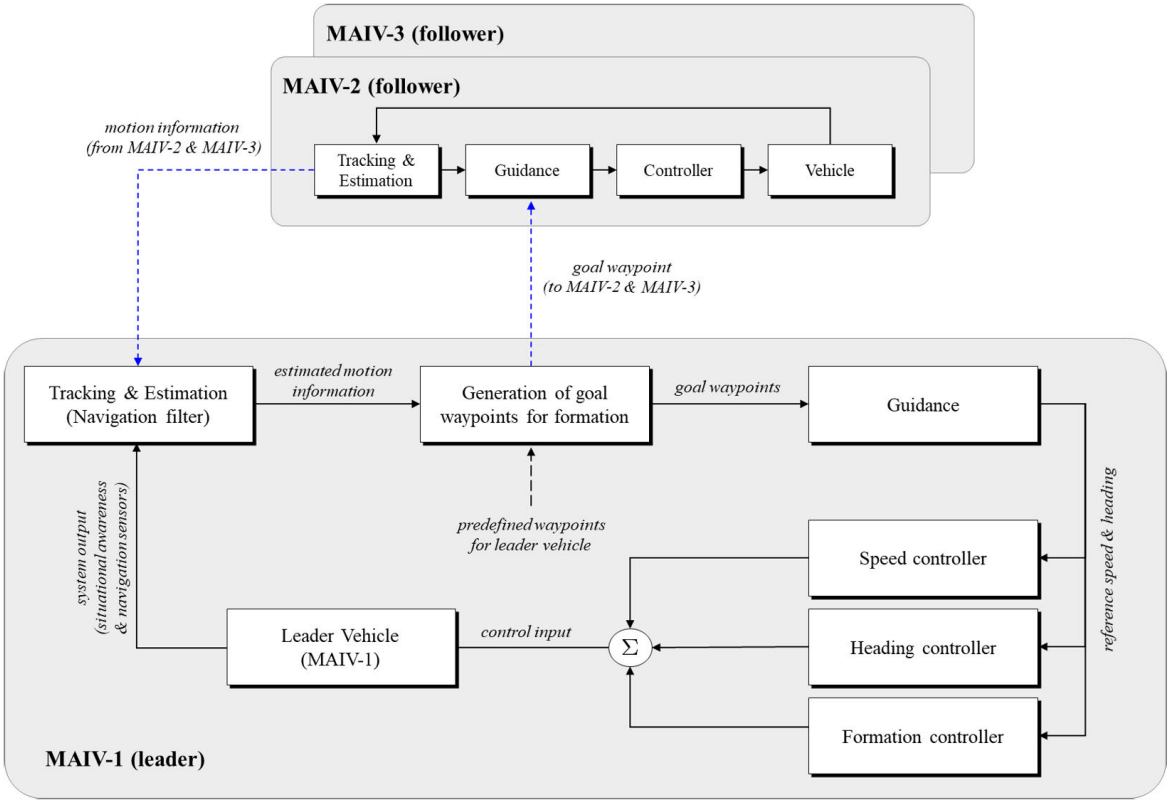

FIGURE 4. Data flow description for the cooperative navigation and control framework. To control the overall operating situation as a leader vehicle, MAIV-1 comprises a tracking and estimation unit for merging motion information from MAIV-2 to N-vehicle.

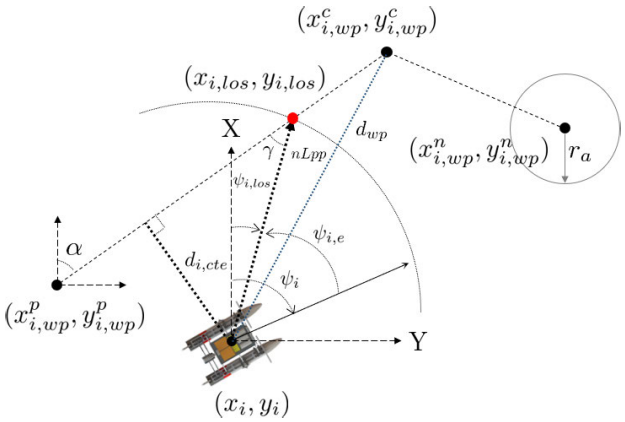

FIGURE 5. Description of guidance laws for waypoint tracking: (x_i, y_i, ψ_i) is the ith vehicle's current motion, and $(x^p_{i,wp}, y^p_{i,wp})$ and $(x^c_{i,wp}, y^c_{i,wp})$ denote the previous and current goal waypoints in the reference coordinate system, respectively.

covariance $\hat{\mathbf{P}}(t)$ corresponding to the predicted state (2) can be obtained as (4).

$$\hat{\mathbf{P}}(t) = \mathbf{F_t}\mathbf{P}(t-1)\mathbf{F_t}^T + \mathbf{B_t}\mathbf{Q}(t)\mathbf{B_t}^T \tag{4}$$

here $\mathbf{F_t}$ and $\mathbf{B_t}$ represent the Jacobian matrices of the kinematic motion model $f(\cdot)$ with respect to the state $\hat{\mathbf{x}}$ and the control input u_t, respectively, and $\mathbf{Q}(t)$ represents the covariance matrix of the control input.

In the correction step of the tracking filter, GNSS was used to correct the predicted motion information using a 3D location (5).

$$\mathbf{z}_{GNSS} = \begin{bmatrix} z_x, & z_y, & z_z \end{bmatrix}^\top \tag{5}$$

Using the measurement of GNSS, the Jacobian matrix corresponding to the measurement model can be represented as (6).

$$\mathbf{H}_t = \begin{bmatrix} \mathbf{I}_{3\times3}, \mathbf{0}_{3\times6} \end{bmatrix} \tag{6}$$

Using the measurement model, the corrected state can be computed using conventional EKF correction equations.

$$\mathbf{x}(t) = \hat{\mathbf{x}}(t) + \mathbf{K}_t(\mathbf{z}_{GNSS}(t) - \hat{\mathbf{z}}_{GNSS}(t)) \tag{7}$$

where $\hat{\mathbf{z}}_{GNSS}$ represents predicted measurement, and $\mathbf{K}$ represents Kalman gain acquired as

$$\mathbf{K}_t = \hat{\mathbf{P}}(t) + \mathbf{H}_t(\mathbf{H}_t\hat{\mathbf{P}}(t)\mathbf{H}_t^T + \mathbf{R}(t))^{-1} \tag{8}$$

where $\mathbf{R}(t)$ represents the covariance matrix of the measurement noise. The corresponding covariance matrix of the corrected state is obtained as

$$\mathbf{P}(t) = (\mathbf{I} - \mathbf{K}_t\mathbf{H}_t)\hat{\mathbf{P}}(t) \tag{9}$$

By following the steps outlined previously, each vehicle can determine its own position and attitude by fusing data from the GNSS and IMU. Fig. 6 illustrates the EKF localization process, which involves fusing the IMU and GNSS for a single vehicle.

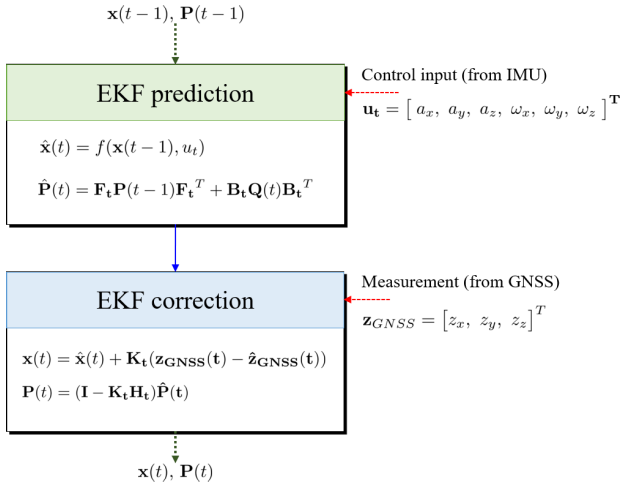

FIGURE 6. EKF localization for a single vehicle by fusing its IMU and GNSS.

2) COOPERATIVE LOCALIZATION USING RELATIVE GEOMETRIC INFORMATION

Because information measured by a single vehicle, as well as relative information between vehicles, can be used, a multi-vehicle system offers advantages in terms of performance efficiency. In particular, a multi-vehicle system can perform given tasks even when the navigation system of a unit vehicle fails. In addition, the proposed approach provided a cooperative localization method using the relative geometric information of vehicles. Each vehicle is assumed equipped with exteroceptive sensors such as radar, LiDAR, and cameras. Vehicles can acquire relative geometric information, such as the range and bearing of other vehicles, using these external sensors. Thus, these sensors can be used to detect other surface objects around the vehicles to identify them and avoid collisions. This study focused on the acquisition of relative geometric information of the developed MAIVs. Furthermore, the framework was designed considering the scalability of the number of vehicles in a multi-vehicle system.

The proposed cooperative localization method was implemented by tracking the motion information of the other vehicles. Each vehicle estimated and tracked the locations of other vehicles using the relative geometric information acquired by external sensors. Moreover, the vehicles in the multi-vehicle system shared the estimated motion information of each vehicle with other vehicles. Through the adoption of the leader–follower concept, each follower vehicle published its estimated motion information, including its own position and attitude toward the leader vehicle. Subsequently, the leader vehicle merged the estimation results of all vehicles in the operating system.

Fig. 4 depicts the data flow for the tracking and estimation processes by merging the motion information of the vehicles. The tracking and estimation processes involved the estimation of motion information and detected objects. In Fig. 4, MAIV-1 was considered the leader vehicle, and other vehicles from 2 to N were used as follower vehicles. The leader and follower vehicles performed localization processes using GNSS and IMU fusion, and the motion information of other vehicles was estimated using external sensors. For simplicity, each vehicle estimated the complete motion information in (1) for itself, whereas only the two-dimensional location (x and y) was estimated for other vehicles. When the ith vehicle detected all other vehicles using its own sensors, the state vector of the estimation was represented as (10)

$$\mathbf{x}_i = \left[\mathbf{x}_{\mathbf{v},i}, \mathbf{x}_1, \cdots, \mathbf{x}_{\mathbf{i-1}}, \mathbf{x}_{\mathbf{i+1}}, \cdots, \mathbf{x}_{\mathbf{N}}\right]^\top \tag{10}$$

where $\mathbf{x}_{\mathbf{v},i}$ represents the 3D full-state vector of the ith vehicle, and $\mathbf{x_j}$ represents the two-dimensional location of the jth vehicle. As previously mentioned, all follower vehicles published the estimated states with covariances to the leader vehicle. The leader vehicle then merged all data, including its own estimated data and that received from the follower vehicles. Thus, it could obtain an accurate estimation for all vehicles. Moreover, if required, the merged data could be published from the leader vehicle in a broadcasting manner to ensure that all maneuvering vehicles had the entire merged data.

Fig. 4 demonstrates an example of the operation of the cooperative navigation framework. In this scenario, MAIV-1 is designated as the leader vehicle and MAIV-2 and MAIV-3 function as follower vehicles. The merged state vector for the leader vehicle (MAIV-1) can be represented as follows:

$$\mathbf{x}_1 = \left[\mathbf{x}_{\mathbf{v},1}, \mathbf{x}_2, \mathbf{x}_3\right]^\top \tag{11}$$

where $\mathbf{x}_{\mathbf{v},1}$ represents the 3D full-state of MAIV-1, and $\mathbf{x}_2$ and $\mathbf{x}_3$ represent the 2D positions of MAIV-2 and MAIV-3, respectively. This enables the leader vehicle (MAIV-1) to estimate the positions and attitudes of the follower vehicles (MAIV-2 and MAIV-3) in addition to its own. As mentioned, the merged data can then be shared with the member vehicles, allowing all vehicles to have access to the same information.

The proposed cooperative localization was achieved using the aforementioned data merging and sharing processes. However, when a follower vehicle of a multi-vehicle system fails to determine its own location, the vehicle must perform localization using the location of other vehicles. The onboard localization system may fail owing to various reasons such as GNSS fault and temporary onboard network failure. This may result in unreliable and inaccurate estimation. In such situations, the vehicle can estimate its own location using the relative geometric information of other vehicles. Thus, a vehicle with onboard localization system failure can perform localization using other vehicles as moving landmarks.

By assuming that all vehicles can merge data via wireless inter-vehicle communication, the cooperative localization problem can be converted to a simple localization problem with a known landmark map. In other words, each vehicle is able to accurately estimate the 2D positions of other vehicles using the data merging process. This means that in the event of an onboard localization failure, a vehicle can still estimate its own location relative to the other vehicles using their accurately estimated positions. The relative geometric

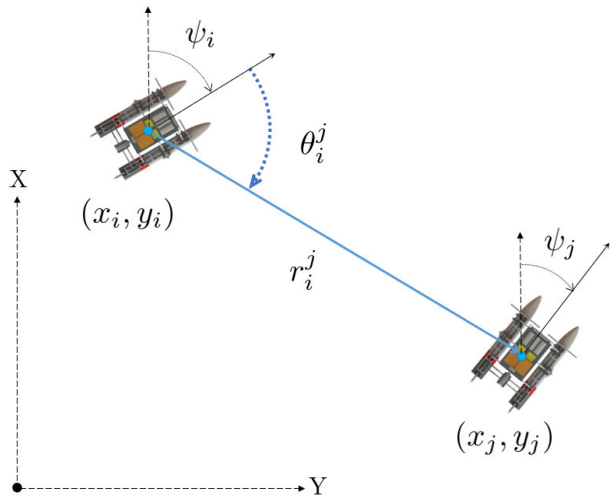

FIGURE 7. Relative geometric information acquisition (range and bearing) between two vehicles.

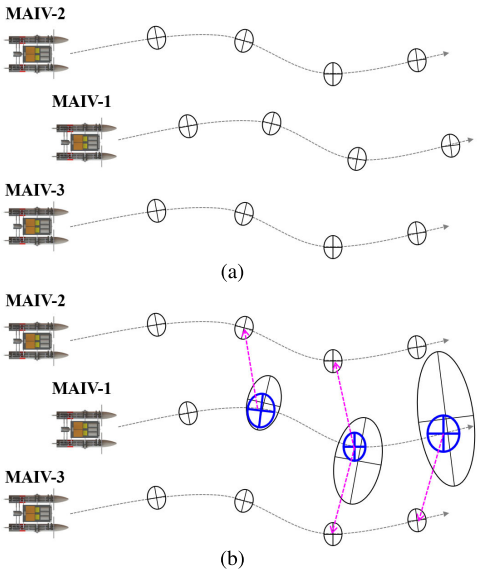

FIGURE 8. Conceptual explanation on cooperative localization. Black ellipses represent the estimates obtained from the onboard localization system, while blue ellipses represent position estimates obtained from cooperative localization when the onboard localization system fails: (a) Three MAIVs perform accurate localization under normal conditions; (b) MAIV-1 experiences an onboard localization system failure but corrects its uncertain position estimation using cooperative localization.

information, which comprises the range and bearing between two vehicles, acquired by the external sensor was used to correct the uncertain location of the vehicle with localization failure. The measurement of the *j*th vehicle with respect to the *i*th vehicle is represented by (12).

$$\mathbf{z}_{ij} = \begin{bmatrix} r_i^j & \theta_i^j \end{bmatrix}^\top \tag{12}$$

here r_i^j and θ_i^j are the relative range and bearing of the *j*th vehicle with respect to the *i*th vehicle, respectively. As previously mentioned, these were acquired from external sensors equipped in the *i*th vehicle. Fig. 7 shows the relative geometric information of the two vehicles. Range r_i^j is defined as the distance between the center points of the two vehicles. Bearing θ_i^j is the relative bearing angle of the *j*th vehicle with respect to the *i*th vehicle.

The measurement model using the measurement in (12) is obtained as follows:

$$\hat{\mathbf{z}}_{ij} = h(\hat{\mathbf{x}}_i) \tag{13}$$

$$= \begin{bmatrix} \sqrt{(x_j - x_i)^2 + (y_j - y_i)^2} \\ \text{atan2}(y_j - y_i, x_j - x_i) - \psi_i \end{bmatrix} \tag{14}$$

Using the aforementioned measurement model, the *i*th vehicle can determine its own location even when the onboard localization sensors fail. Consequently, the multi-vehicle system can continue to perform a particular task using the proposed cooperative localization processes.

Fig. 8 illustrates the proposed cooperative localization approach. Under normal conditions, all three vehicles can accurately estimate their positions by fusing GNSS and IMU data. However, if MAIV-1 suffers from GNSS fault, it cannot perform accurate self-localization using its onboard system, producing inaccurate and highly uncertain results. In such a case, MAIV-1 can leverage LiDAR sensors to detect MAIV-2 or MAIV-3 and use the relative geometric information to correct its own position estimation by incorporating the location of other MAIVs.

C. COOPERATIVE FORMATION CONTROL

1) FORMATION CONTROL BASED ON THE ARTIFICIAL POTENTIAL FIELD APPROACH

While each vehicle maneuvers toward each aiming waypoint, a conflict between vehicles may occur. To prevent and resolve this conflict, the potential field approach based on two types of relative distances, that is, the distance between vehicles and the distance from a vehicle to the predefined goal waypoint was used, as shown in Fig. 9. By defining an appropriate potential field function [42], [43], the potential field force was derived and employed as a control input in the designed control framework of each vehicle. Herein, the predefined potential field function was assumed differentiable over a specific interval. The potential field function related to the potential force could then be expressed as $F(q_v, q_{wp}) = -\nabla U(q_v, q_{wp})$. Furthermore, $\nabla U(q_v, q_{wp})$ was defined as the gradient vector of the potential field function (U), which could be defined as the sum of attractive and repulsive field functions, as follows:

$$U(q_v, q_{wp}) = U_{att}(q_v, q_{wp}) + U_{rep}(r(q_v)) \tag{15}$$

where q_{wp} denotes the goal waypoint (x_{wp}^c, y_{wp}^c) of the assigned vehicle, q_v denotes the vehicle position (x, y), and $r(q_v)$ denotes the Euclidean distance between the vehicle and its neighboring vehicle. For example, the distance between the *i*th and *j*th vehicles is defined as $r_i^j(q_{i,v}) \equiv r_j^i(q_{j,v})$.

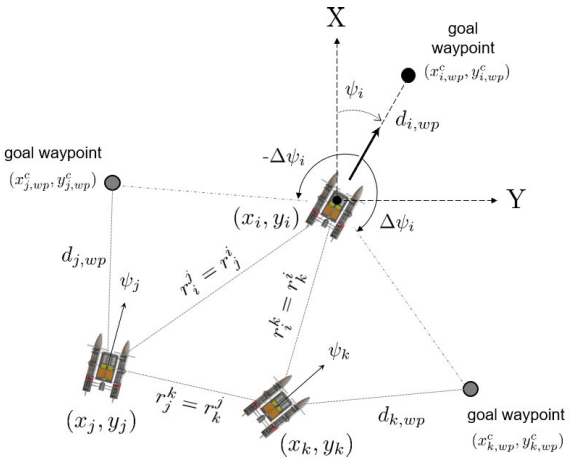

FIGURE 9. Proposed formation control scheme.

The potential field force can be divided into attractive and repulsive forces as follows:

$$F(q_v, q_{wp}) = F_{att}(q_v, q_{wp}) + F_{rep}(q_v) = -\nabla U_{att}(q_v, q_{wp}) - \nabla U_{rep}(r(q_v)) \quad (16)$$

The attractive potential function is expressed as

$$U_{att}(q_v, q_{wp}) = \frac{1}{2} k_\alpha (d^2_{wp}(q_v, q_{wp})) \quad (17)$$

where k_α is a positive scalar control factor and $d_{wp}(q_v, q_{wp})$ denotes the Euclidean distance between the vehicle and its goal waypoint. For example, the distance between the ith vehicle and its goal waypoint is $d^{i,wp}(q_{i,v}, q_{i,wp})$.

The repulsive potential function is defined as

$$U_{rep}(r(q_v)) = \begin{cases} k_\beta(\ln(r(q_v)) + \dfrac{r_{\min}}{r(q_v)}) & r_{\min} < r(q_v) < r_{\max} \\ k_\beta(\ln(r_{\max}) + \dfrac{r_{\min}}{r_{\max}}) & r(q_v) \geq r_{\max} \end{cases} \quad (18)$$

where k_β denotes the scalar control factor. In addition, $r_{\max}$ and $r_{\min}$ denote the maximum and minimum distances influenced by the other vehicle, respectively.

2) VEHICLE CONTROL TO FOLLOW THE PROPOSED GUIDANCE LAWS AND FORMATION CONTROL SCHEME

To control the heading angle and speed of each vehicle along the desired waypoints, a conventional proportional-derivative (PD) controller was designed and implemented using the LOS and CT guidance approaches. The control input for the vehicle autopilot is defined as $\mathbf{u} = \mathbf{u}_0 + \mathbf{u}_{gc} + \mathbf{u}_{fc}$. $\mathbf{u}_0$ denotes the control input for the nominal cruising speed of the vehicle. Considering the LOS and CT guidance approaches, the control input is designed as

$$\mathbf{u}_{gc} = \rho(k^p_{los}\psi_e + k^d_{los}\dot{\psi}_e) + (1-\rho)(k^p_{cte}d_{cte} + k^d_{cte}\dot{d}_{cte}) \quad (19)$$

here, $k^p_{\{\cdot\}}$ and $k^d_{\{\cdot\}}$ are the proportional and differential gain coefficients, respectively, which determine the weight of the transfer factors and consider the units of errors. The ratio of the relative distance, denoted by ρ, represents the distance between $(x^p_{i,wp}, y^p_{i,wp})$ and $(x^c_{i,wp}, y^c_{i,wp})$ relative to the distance from (x_i, y_i) to $(x^c_{i,wp}, y^c_{i,wp})$. ρ is adaptively used as the weight factor, and if it larger than 1, it is set to 1. Further, the control input for formation control u_{fc} on the ith vehicle is expressed as

$$\mathbf{u}_{i,fc} = F_{att}(q_{i,v}, q_{i,wp}) + F_{rep}(q_{i,v}) = -\nabla U_{att}(q_{i,v}, q_{i,wp}) - \sum_{i \neq j}^{n} \nabla U_{rep}(r^j_i(q_{i,v})) \quad (20)$$

When another vehicle was within a certain radius of each vehicle, the control input generated by the resultant force was reflected to prevent and release conflicts between vehicles in the designed control framework.

IV. FIELD EXPERIMENTS

This section describes the experimental results of the preliminary field tests conducted in an inland water environment. The aim was to demonstrate the feasibility of the developed system and designed autonomous cooperative navigation and control framework. Various field tests were conducted in the waters near Jangseong Lake, and the GCS was located to simultaneously operate, control, and monitor the developed MAIVs, as shown in Fig. 10. Moreover, the proposed GNC algorithms were implemented to confirm the operational stability and reliability of the developed system. To validate the feasibility of the proposed relative geometric information-based navigation approach, a test was performed to estimate the motion information using only the LiDAR-estimated information by considering a situation where GNSS was not received. In addition, several field tests for validating the proposed cooperative formation control scheme were conducted considering two types of formations: longitudinal and triangular.

A. WAYPOINT GUIDANCE AND TRACKING CONTROL

The field test results corresponding to each vehicle implemented with the proposed GNC approach are shown in Fig. 11. The nominal cruising speed of each MAIV was set to approximately 3–5 knots and the circle of acceptance radius for each waypoint was set to 2.5L. Under nominal cruising operation conditions, the root mean square error (RMSE) of the cross-track was approximately within 1.5L on average for each MAIV, except for the turning sections when altering the goal waypoint. In addition, the turning radius with respect to the port and starboard directions of each vehicle was approximately within 3L. These maneuvering performance test results prove the feasibility of the proposed GNC approach.

B. MAIV COOPERATIVE NAVIGATION AND LOCALIZATION

Inland field tests were performed to verify the performance of the proposed cooperative localization method. The MAIVs were controlled to follow a particular path by maintaining

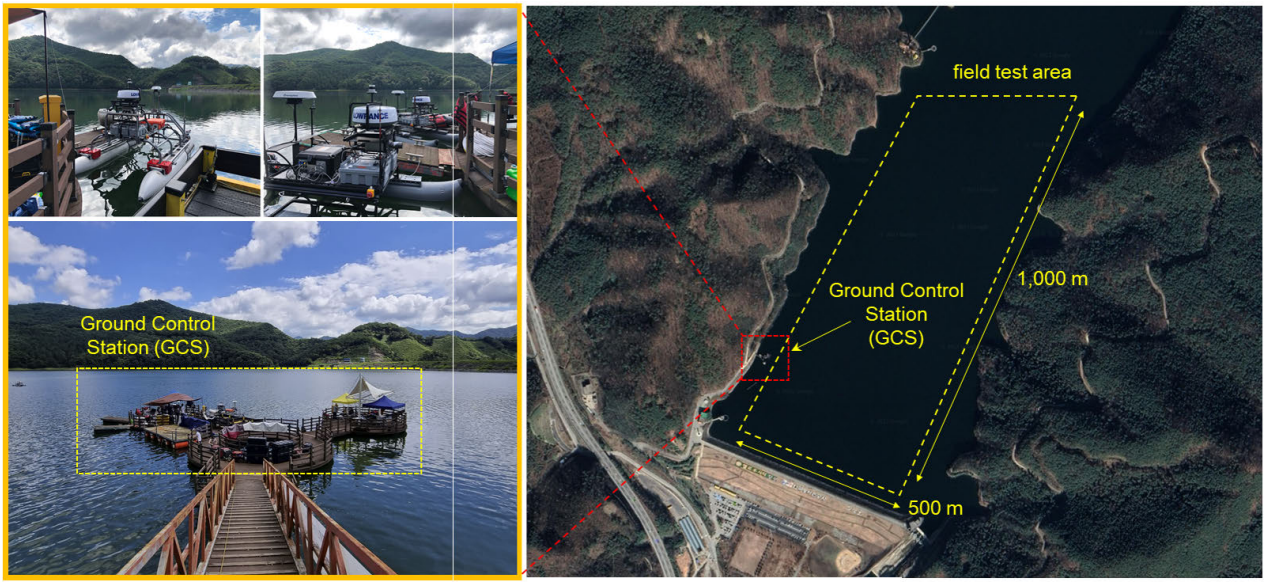

FIGURE 10. Test site images of Jangseong Lake, Jangseong-gun, Republic of Korea, overlaid with an area wherein the field tests were conducted and the ground control station (GCS) for operating and controlling the MAIVs. The field test area was set considering the wireless communication range (approximately up to 750–800 m).

their relative formation. MAIV-1 was considered as the leader vehicle, and the other two vehicles followed it up to a certain distance. The network systems of all MAIVs were connected via wireless communication to facilitate sharing the estimation results between vehicles. Fig. 12 shows the location of the GCS and true trajectories of the three MAIVs. The MAIVs maneuvered from south to north. The three MAIVs exhibited complex motions around the starting points because they were initially located at arbitrary positions and heading directions. After passing the first waypoints defined as starting locations, the MAIVs maneuvered forward by following the given goal waypoints while maintaining a relative formation.

1) RELATIVE GEOMETRIC INFORMATION ACQUISITION

As a preliminary test, a field test without objects other than the three MAIVs was conducted. The onboard LiDAR (Ouster, OS1-64) was used to acquire the relative geometric information between the two vehicles because they were operated within the LiDAR detection range. Further, to estimate the relative range and bearing between the two vehicles using a LiDAR sensor, the procedure was divided into three phases. The first was the filtering process phase, wherein a voxel grid filtering technique was employed to enhance the computing efficiency and minimize inherent noises (e.g., a reflection of water and wake) induced in the marine environment and outliers over the point cloud data. Subsequently, the density-based spatial clustering of applications with noise (DBSCAN) method [44] was applied to identify objects with an arbitrary shape, such as vessels and buoys, in the marine environment. This method is a highly efficient clustering approach for large spatial point cloud data. Finally, in the closing phase, using the clustered objects, the relative distance and bearing information were calculated from the center point of the clustered point clouds.

2) RESULTS OF THE PROPOSED APPROACH

To test the performance of the cooperative navigation and localization method, the GNSS failure situation was simulated in MAIV-1 without using GNSS data. The simulated GNSS failure ranged from 200 to 290 s. During the GNSS failure, MAIV-1 performed cooperative navigation and localization processes. It acquired relative geometric information for both MAIV-2 and MAIV-3 using its onboard LiDAR sensor. The cameras and radar could also be used to detect other vehicles. However, three MAIVs were closely located during the test; thus, the LiDAR could be more effective in acquiring relative geometric information.

Fig. 13 presents the estimated results for the three MAIVs. Because MAIV-2 and MAIV-3 could reliably localize using GNSS and IMU, their estimated locations showed accurate results. The experimental results, as shown in Fig. 13, indicate that MAIV-1 estimates its own location even when GNSS was not available, as mentioned previously. The cooperative navigation and localization performance was evaluated using the localization error. Fig. 14 shows the estimation errors for MAIV-1. When an onboard GNSS was available, the estimated error was less than 0.2 m for most of the experimental period. The estimation error was larger than 0.5 m for two main periods: 50–120 and 200–290 s. The first was not induced by GNSS failure. At 50–120 s, the monitoring boat maneuvered closer to MAIV-2. Further, LiDAR detection confused the monitored boat with MAIV-2; therefore, incorrect detection resulted in an estimation error. During the GNSS failure, which ranged from 200 to 290 s, the error increased to approximately 1.0 m. Although the estimation error was larger than the normal condition of GNSS-based

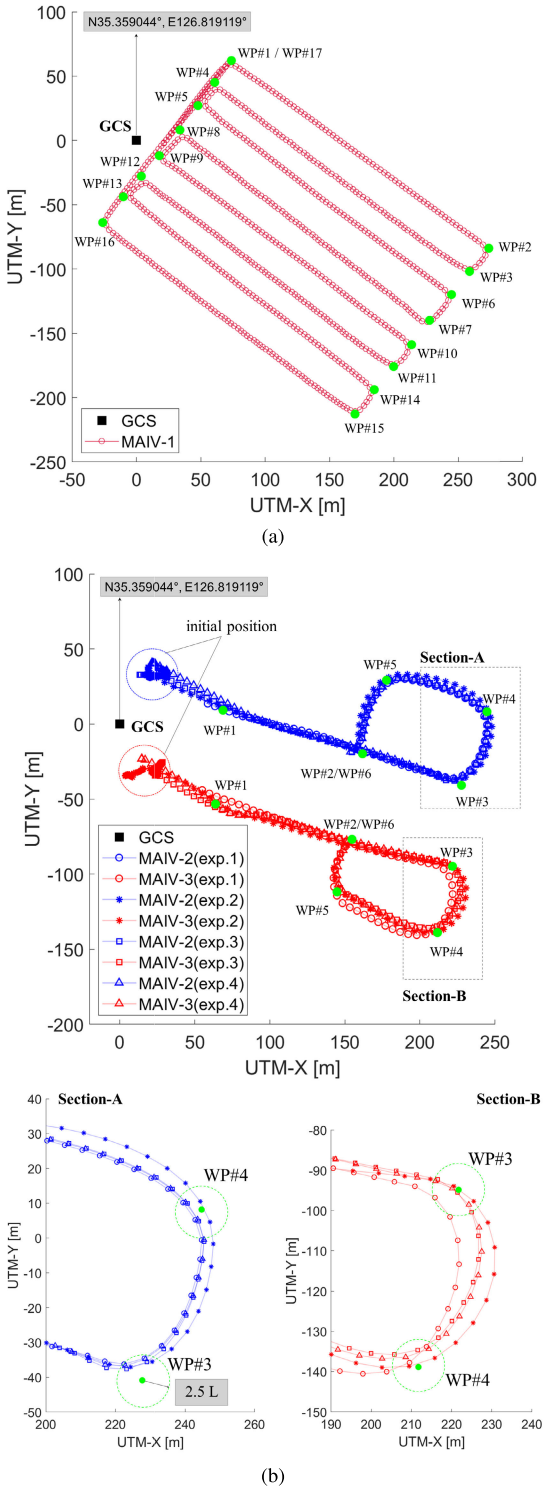

FIGURE 11. Results for the proposed GNC approach: (a) Field test of MAIV-1; (b) Field tests with respect to MAIV-2 and MAIV-3.

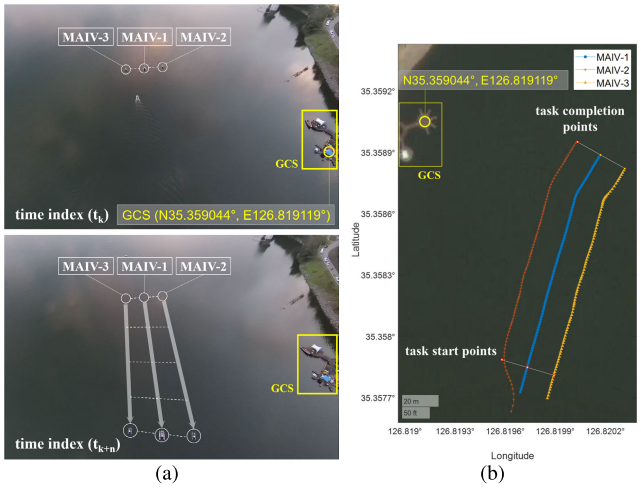

FIGURE 12. Cooperative navigation and localization scenario: (a) Snapshots of the MAIV maneuvering trajectories; (b) Trajectories of the MAIVs that maneuvered while maintaining an arbitrary longitudinal formation.

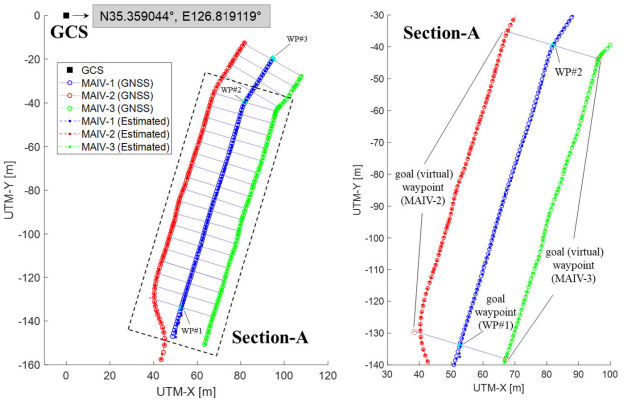

FIGURE 13. Trajectory estimated by the proposed cooperative localization method compared with the true trajectory of MAIV-1.

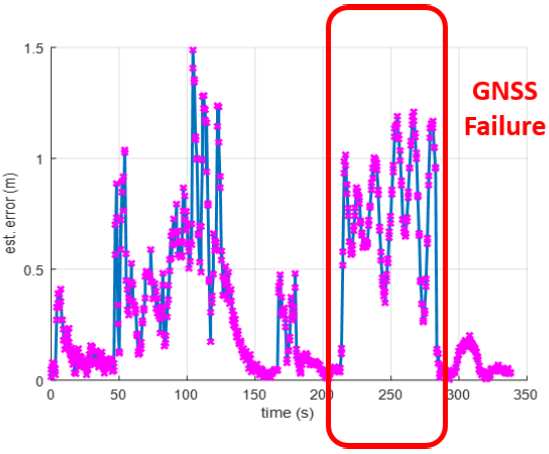

FIGURE 14. Estimated error for MAIV-1 that was simulated with GNSS failure.

localization, it did not diverge and was bounded by less than 1.2 m. Thus, the experimental results show that the proposed method can provide a reliable estimation of the cooperative navigation and localization system, despite detection errors and GNSS failure.

C. COOPERATIVE GUIDANCE AND FORMATION CONTROL

Two types of field tests were conducted to demonstrate the proposed cooperative formation control scheme. Fig. 15

FIGURE 15. Snapshots for autonomous cooperative formation tasks for MAIVs.

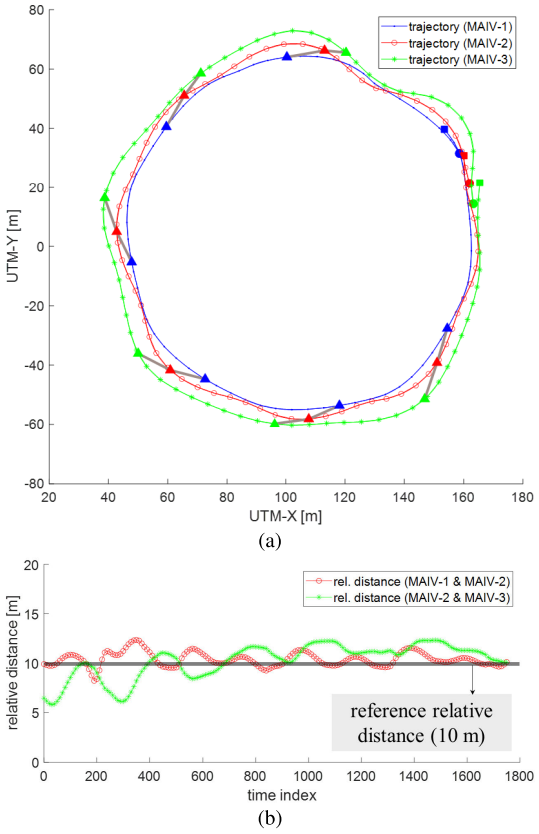

FIGURE 16. Result for maintaining a longitudinal geometric formation of the proposed formation control scheme: (a) Trajectories of the MAIVs that maneuvered while maintaining an arbitrary longitudinal formation; (b) Time history of the relative distance between MAIV-1 and MAIV-2 (red dot line) and between MAIV-2 and MAIV-3 (green star line).

shows the field test results for maintaining the relative distance between the vehicles in a row. In these tests, the leader vehicle (i.e., MAIV-1) maneuvered at a constant speed toward the predefined waypoint, and the follower vehicles

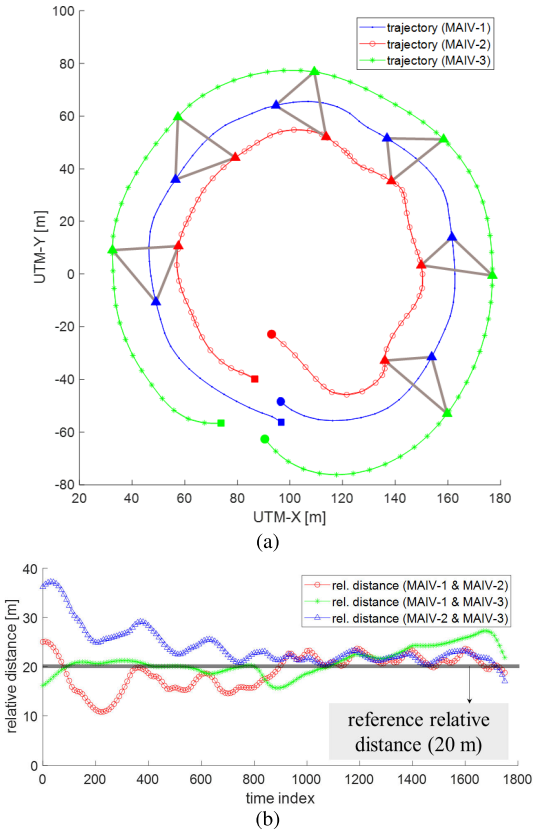

FIGURE 17. Result for maintaining a triangular geometric formation of the proposed formation control scheme: (a) Trajectories of the MAIVs that maneuvered while maintaining an arbitrary triangular formation; (b) Time history of the relative distance between MAIV-1 and MAIV-2 (red dot line, RMSE for the relative distance: 3.52 m), between MAIV-1 and MAIV-3 (green star line, RMSE for the relative distance: 2.89 m), and between MAIV-2 and MAIV-3 (blue upward-pointing triangle line, RMSE for the relative distance: 5.53 m).

(i.e., MAIV-2 and MAIV-3) were controlled to follow the generated waypoints considering the variation in maneuvering speed depending on the relative distance. As shown in Fig. 16, based on MAIV-1, a test was performed to maneuver at a specific interval in the longitudinal geometric formation. Herein, the interval between the vehicles was set to 10 m. In Fig. 16(b), the RMSEs of the relative distances between MAIV-1 and MAIV-2 and between MAIV-2 and MAIV-3 were evaluated as 0.81 and 1.72 m, respectively. The RMSE of MAIV-3, located at the rear of the formation, was relatively large. This may be because MAIV-3 was affected by the disturbance caused by a wake generated behind MAIV-1 and MAIV-2.

Furthermore, a test for maintaining a triangular geometric formation was performed, as shown in Fig. 17. An arbitrary triangular formation was built to maintain the relative distance, which was set to 20 m. As mentioned previously, MAIV-2 and MAIV-3 may be affected by the wake generated by MAIV-1. In addition, it appeared that because the vehicles were close together in the triangular geometric formation, mutual repulsive forces occurred, resulting in relative chattering in the proposed potential field force. Nevertheless, the

MAIVs were controlled to maintain a particular geometric formation over time at their initial location.

V. CONCLUSION

The development and field testing of multiple MAIVs, developed by KRISO, for autonomous cooperative navigation tasks are presented. For reliable operation and control of the MAIVs without unstable network latency, the network architecture and configuration were fundamentally designed, and they enabled the sharing of motion information. In addition, a framework for cooperative navigation that considered a formation control scheme is proposed. In particular, to deal with GNSS failure in the MAIVs, a cooperative navigation and localization approach is proposed using the relative geometric information between other vehicles. Moreover, preliminary field tests were conducted in an inland water environment to demonstrate the reliability and feasibility of the developed MAIVs and proposed framework. The test results successfully verified the reliability and feasibility of the developed system and the operational algorithms implemented in the proposed cooperative navigation and control framework.

The proposed control and localization framework has demonstrated successful performance using the kinematic model of MAIVs. However, to achieve an even more precise control in the presence of ocean waves and currents, future studies will extend the proposed framework to include not only the kinematic model but also the dynamic model of the vehicles. Future research may also focus on simultaneously fusing and merging all motion and situational awareness information obtained from follower MAIVs in the leader MAIV. Furthermore, fault- and detection-related research will be conducted to implement fault diagnosis functions, including whether any vehicle is in abnormal operation and maneuvering condition. These could help provide optimal and robust mission performance using a group of vehicles under unfavorable environmental conditions for various mission tasks.

REFERENCES

[1] C. A. Thieme and I. B. Utne, "Safety performance monitoring of autonomous marine systems," *Rel. Eng. Syst. Saf.*, vol. 159, pp. 264–275, Mar. 2017.
[2] S. Themann, "New autonomous systems needed to meet future demand for marine data," *Hydrographic Notices*, vol. 122, pp. 30–32, Jan. 2022.
[3] H. Xu, L. Moreira, and C. G. Soares, "Maritime autonomous vessels," *J. Mar. Sci. Eng.*, vol. 11, no. 1, p. 168, Jan. 2023.
[4] Z. Liu, Y. Zhang, X. Yu, and C. Yuan, "Unmanned surface vehicles: An overview of developments and challenges," *Annu. Rev. Control*, vol. 41, pp. 71–93, Jan. 2016.
[5] E. Simetti, G. Indiveri, and A. M. Pascoal, "WiMUST: A cooperative marine robotic system for autonomous geotechnical surveys," *J. Field Robot.*, vol. 38, no. 2, pp. 268–288, Mar. 2021.
[6] Y. Singh, "Cooperative swarm optimisation of unmanned surface vehicles," School Eng., Univ. Plymouth, Plymouth, U.K., 2019.
[7] S. H. Juan and F. H. Cotarelo, "Multi-master ROS systems," Institut de Robòtica i Informàtica Ind., Tech. Rep., 2015.
[8] A. Tiderko, F. Hoeller, and T. Röhling, "The ROS multimaster extension for simplified deployment of multi-robot systems," in *Robot Operating System (ROS)*. Cham, Switzerland: Springer, 2016, pp. 629–650.
[9] P. Anggraeni, M. Mrabet, M. Defoort, and M. Djemai, "Development of a wireless communication platform for multiple-mobile robots using ROS," in *Proc. 6th Int. Conf. Control Eng. Inf. Technol. (CEIT)*, Oct. 2018, pp. 1–6.
[10] M. Garzón, J. Valente, J. J. Roldán, D. Garzón-Ramos, J. de. León, A. Barrientos, and J. del Cerro, "Using ROS in multi-robot systems: Experiences and lessons learned from real-world field tests," in *Robot Operating System (ROS)*. Cham, Switzerland: Springer, 2017, pp. 449–483.
[11] Z. Peng, J. Wang, D. Wang, and Q.-L. Han, "An overview of recent advances in coordinated control of multiple autonomous surface vehicles," *IEEE Trans. Ind. Informat.*, vol. 17, no. 2, pp. 732–745, Jun. 2021.
[12] J. Zhao, Y. Zhang, S. Ni, and Q. Li, "Bayesian cooperative localization with NLOS and malicious vehicle detection in GNSS-challenged environments," *IEEE Access*, vol. 8, pp. 85686–85697, 2020.
[13] J. Han, J. Park, J. Kim, and N.-S. Son, "GPS-less coastal navigation using marine radar for USV operation," *IFAC-PapersOnLine*, vol. 49, no. 23, pp. 598–603, 2016.
[14] A. Felski and K. Zwolak, "The ocean-going autonomous ship—Challenges and threats," *J. Mar. Sci. Eng.*, vol. 8, no. 1, p. 41, Jan. 2020. [Online]. Available: https://www.mdpi.com/2077-1312/8/1/41
[15] F. Massa, L. Bonamini, A. Settimi, L. Pallottino, and D. Caporale, "LiDAR-based GNSS denied localization for autonomous racing cars," *Sensors*, vol. 20, no. 14, p. 3992, Jul. 2020.
[16] Y. Tobata, R. Kurazume, Y. Iwashita, and T. Hasegawa, "Automatic laser-based geometrical modeling using multiple mobile robots," in *Proc. IEEE Int. Conf. Robot. Biomimetics*, Dec. 2010, pp. 363–369.
[17] S. Hood, K. Benson, P. Hamod, D. Madison, J. M. O'Kane, and I. Rekleitis, "Bird's eye view: Cooperative exploration by UGV and UAV," in *Proc. Int. Conf. Unmanned Aircr. Syst. (ICUAS)*, Jun. 2017, pp. 247–255.
[18] D. Wang, B. Lian, and C. Tang, "UGV-UAV robust cooperative positioning algorithm with object detection," *IET Intell. Transp. Syst.*, vol. 15, no. 7, pp. 851–862, Jul. 2021.
[19] V. P. Bacheti, A. S. Brandao, and M. Sarcinelli-Filho, "A path-following controller for a UAV-UGV formation performing the final step of last-mile-delivery," *IEEE Access*, vol. 9, pp. 142218–142231, 2021.
[20] G. Rui and M. Chitre, "Cooperative multi-AUV localization using distributed extended information filter," in *Proc. IEEE/OES Auto. Underwater Vehicles (AUV)*, Nov. 2016, pp. 206–212.
[21] F. Mason, F. Chiariotri, F. Campagnaro, A. Zanella, and M. Zorzi, "Low-cost AUV swarm localization through multimodal underwater acoustic networks," in *Proc. Global Oceans, Singapore U.S. Gulf Coast*, Oct. 2020, pp. 1–7.
[22] R. Ren, L. Zhang, L. Liu, D. Wu, G. Pan, Q. Huang, Y. Zhu, Y. Liu, and Z. Zhu, "Multi-AUV cooperative navigation algorithm based on temporal difference method," *J. Mar. Sci. Eng.*, vol. 10, no. 7, p. 955, Jul. 2022. [Online]. Available: https://www.mdpi.com/2077-1312/10/7/955
[23] Y. Yao, "Cooperative navigation system for multiple unmanned underwater vehicles," *IFAC Proc. Volumes*, vol. 46, no. 20, pp. 719–723, 2013. [Online]. Available: https://www.sciencedirect.com/science/article/pii/S1474667016316226
[24] G. Salavasidis, C. Harris, E. Rogers, and A. Phillips, "Co-operative use of marine autonomous systems to enhance navigational accuracy of autonomous underwater vehicles," in *Proc. Annu. Conf. Towards Auton. Robotic Syst.*, vol. 9716, Jun. 2016, pp. 275–281.
[25] L. Ma, Y.-L. Wang, and Q.-L. Han, "Cooperative target tracking of multiple autonomous surface vehicles under switching interaction topologies," *IEEE/CAA J. Autom. Sinica*, vol. 10, no. 3, pp. 673–684, Mar. 2023.
[26] M. F. Fallon, G. Papadopoulos, J. J. Leonard, and N. M. Patrikalakis, "Cooperative AUV navigation using a single maneuvering surface craft," *Int. J. Robot. Res.*, vol. 29, no. 12, pp. 1461–1474, Oct. 2010.
[27] J. Qu, X. Li, and G. Sun, "Optimal formation configuration analysis for cooperative localization system of multi-AUV," *IEEE Access*, vol. 9, pp. 90702–90714, 2021.
[28] J. M. Soares, A. P. Aguiar, A. M. Pascoal, and M. Gallieri, "Triangular formation control using range measurements: An application to marine robotic vehicles," *IFAC Proc. Volumes*, vol. 45, no. 5, pp. 112–117, 2012.
[29] Y. Liu and R. Bucknall, "A survey of formation control and motion planning of multiple unmanned vehicles," *Robotica*, vol. 36, no. 7, pp. 1019–1047, Jul. 2018.
[30] L. Consolini, F. Morbidi, D. Prattichizzo, and M. Tosques, "Leader-follower formation control of nonholonomic mobile robots with input constraints," *Automatica*, vol. 44, no. 5, pp. 1343–1349, May 2008.

[31] M. Breivik, V. E. Hovstein, and T. I. Fossen, "Ship formation control: A guided leader-follower approach," *IFAC Proc. Volumes*, vol. 41, no. 2, pp. 16008–16014, 2008.
[32] A. S. Simonsen and E.-L.-M. Ruud, "The application of a flexible leader-follower control algorithm to different mobile autonomous robots," in *Proc. IEEE/RSJ Int. Conf. Intell. Robots Syst. (IROS)*, Oct. 2020, pp. 11561–11566.
[33] H. Mehrjerdi, J. Ghomman, and M. Saan, "Nonlinear coordination control for a group of mobile robots using a virtual structure," *Mechatronics*, vol. 21, no. 7, pp. 1147–1155, Oct. 2011.
[34] M. Bibuli, A. Gasparri, A. Priolo, G. Bruzzone, and M. Caccia, "Virtual target based path-following guidance system for cooperative USV swarms," *IFAC Proc. Volumes*, vol. 45, no. 27, pp. 362–367, 2012.
[35] H. Rezaee and F. Abdollahi, "A decentralized cooperative control scheme with obstacle avoidance for a team of mobile robots," *IEEE Trans. Ind. Electron.*, vol. 61, no. 1, pp. 347–354, Jan. 2014.
[36] T. Balch and R. C. Arkin, "Behavior-based formation control for multirobot teams," *IEEE Trans. Robot. Autom.*, vol. 14, no. 6, pp. 926–939, Dec. 1998.
[37] G. Lee and D. Chwa, "Decentralized behavior-based formation control of multiple robots considering obstacle avoidance," *Intell. Service Robot.*, vol. 11, no. 1, pp. 127–138, 2018.
[38] K.-K. Oh, M.-C. Park, and H.-S. Ahn, "A survey of multi-agent formation control," *Automatica*, vol. 53, pp. 424–440, Mar. 2014.
[39] N. R. Rypkema and H. Schmidt, "Formation control of a drifting group of marine robotic vehicles," in *Distributed Autonomous Robotic Systems*. Cham, Switzerland: Springer, 2018, pp. 633–647.
[40] X. Sun, G. Wang, Y. Fan, D. Mu, and B. Qiu, "A formation collision avoidance system for unmanned surface vehicles with leader-follower structure," *IEEE Access*, vol. 7, pp. 24691–24702, 2019.
[41] X. Zhou, P. Wu, H. Zhang, W. Guo, and Y. Liu, "Learn to navigate: Cooperative path planning for unmanned surface vehicles using deep reinforcement learning," *IEEE Access*, vol. 7, pp. 165262–165278, 2019.
[42] O. Khatib, "Real-time obstacle avoidance for manipulators and mobile robots," in *Proc. IEEE Int. Conf. Robot. Autom.*, vol. 2, Mar. 1985, pp. 500–505.
[43] N. E. Leonard and E. Fiorelli, "Virtual leaders, artificial potentials and coordinated control of groups," in *Proc. 40th IEEE Conf. Decision Control*, vol. 3, Dec. 2001, pp. 2968–2973.
[44] M. Ester, H. P. Kriegel, J. Sander, and X. Xu, *A Density-Based Algorithm for Discovering Clusters in Large Spatial Databases With Noise*. Palo Alto, CA, USA: AAAI Press, 1996, pp. 226–231.

JEONGHONG PARK (Member, IEEE) received the B.S. and M.S. degrees in mechatronics engineering from Chungnam National University, Daejeon, South Korea, in 2005 and 2007, respectively, and the Ph.D. degree in mechanical engineering from the Korea Advanced Institute of Science and Technology (KAIST), Daejeon, in 2016. He is currently a Senior Researcher with the Korea Research Institute of Ships and Ocean Engineering (KRISO), Daejeon. His research interests include ocean robotics, intelligent situational awareness, multi-agent cooperative navigation, and collision-free path planning of autonomous ships and marine robots.

MINJU KANG (Member, IEEE) received the B.S. degree in mechanical engineering and the M.S. degree in ocean system engineering from the Korea Advanced Institute of Science and Technology (KAIST), Daejeon, South Korea, in 2014 and 2016, respectively. He was a Researcher at the Korea Electrotechnology Research Institute (KERI), from 2016 to 2020. He is currently a Researcher with the Korea Research Institute of Ships and Ocean Engineering (KRISO), Daejeon. His current research interests include autonomous and intelligent maritime systems.

YEONGJUN LEE (Member, IEEE) received the B.S. and M.S. degrees in mechatronics engineering from Chungnam National University, Daejeon, South Korea, in 2009 and 2014, respectively. He is currently a Senior Engineer with the Korea Research Institute of Ships and Ocean Engineering (KRISO), Daejeon. His current research interests include acoustic image recognition, sonar-based localization, and underwater laser scanning system for marine robotic systems.

JONGDAE JUNG (Member, IEEE) received the B.S. degree in civil engineering from Hanyang University, Seoul, South Korea, in 2008, and the M.S. and Ph.D. degrees in civil and environmental engineering from the Korea Advanced Institute of Science and Technology (KAIST), Daejeon, South Korea, in 2010 and 2015, respectively. From 2016 to 2022, he was a Senior Researcher with the Korea Research Institute of Ships and Ocean Engineering (KRISO), Daejeon. Since 2022, he has been an Assistant Professor with the Department of Naval Architecture and Ocean Engineering, Chungnam National University, Daejeon. His current research interests include autonomous navigation of marine robots, intelligent maritime systems, and multi-agent mission planning.

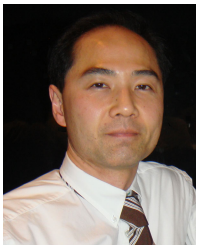

HYUN-TAEK CHOI (Member, IEEE) received the B.S., M.S., and Ph.D. degrees in electronic engineering from Hanyang University, Seoul, South Korea, in 1991, 1993, and 2000, respectively. He was an Associate Research Engineer with Korea Telecom, from 1993 to 1995. He was a Postdoctoral Researcher with the University of Hawai'i, from 2000 to 2003. He is currently a Principal Researcher with the Korea Research Institute of Ships and Ocean Engineering (KRISO), Daejeon, South Korea. He has been leading various projects related to marine robotic applications, such as ROVs, AUVs, USVs, and autonomous ships.

JINWOO CHOI (Member, IEEE) received the B.S., M.S., and Ph.D. degrees in mechanical engineering from the Pohang University of Science and Technology (POSTECH), South Korea, in 2003, 2005, and 2011, respectively. He is currently a Principal Researcher with the Korea Research Institute of Ships and Ocean Engineering (KRISO), Daejeon, South Korea. His current research interests include mapping, localization, SLAM, and acoustic source localization for marine robots.